

# Mathematical Simulation of Calcimine Deliming in the Production of Gelatin

Karel Kolomazník

Tomas Bata University, Faculty of Applied Informatics, Nad Stráněmi 4511, 760 05 Zlín, Czech Republic

Tomáš Fürst

Dept. of Mathematical Analysis and Applications of Mathematics, Faculty of Science,  
Palacký University in Olomouc, Tr. Svobody 26, 779 00 Olomouc, Czech Republic

Michaela Bařinová

Tomas Bata University, Faculty of Applied Informatics, Nad Stráněmi 4511, 760 05 Zlín, Czech Republic

DOI 10.1002/aic.12069

Published online March 22, 2010 in Wiley InterScience (www.interscience.wiley.com).

*Calcimine is a valuable by-product originating during the processing of cured hide into leather. It is used as raw material in the production of gelatin and biodegradable sheets. For further usage, it is necessary to remove calcium hydroxide from calcimine by chemical deliming, which is, from the environmental protection point of view, the most important stage of the entire deliming process. In this article, a mathematical description of chemical deliming is proposed, based on the unreacted nucleus approach. Numerical solution of the model is found, concentration fields of the reacting chemicals described, and the evolution of the acido-basic boundary inside calcimine shown. The model is used to justify a simplified way to determine the effective diffusion coefficient of the deliming agent. The model can also be used as a basis for optimization of the deliming process. © 2010 American Institute of Chemical Engineers*

*Keywords:* mathematical modeling, deliming, diffusion, unreacted nucleus, free boundary

## Introduction

Limed collagen splits (hereafter referred to as calcimine) represent a valuable by-product originating during the processing of cured hide into leather. It is produced in the dehairing stage which follows the soaking operation. In the dehairing process, sodium sulphide reduces cysteine—the dominant amino-acid present in keratin—to cystine, which is accompanied by the destruction of the keratin protein. The result of the operation is the so-called white hide. The dehairing process takes place in a strongly alkaline ambience

of calcium hydroxide (lime). After this stage, parts of white hide are cut off in order to facilitate further mechanical treatment of the dehaired hide. These so-called calcimine splits become valuable raw material for the production of gelatin and hide-mucilage.

Before being further processed, calcimine is soaked in technological water containing detergents in order to remove sodium sulphide. The soaking operation is followed by liming, which takes place in an aqueous solution of calcium hydroxide in underground concrete pits, to reduce the molar mass of the collagen protein. The duration of this operation is controlled by measuring the contents of amidic nitrogen. Depending on the ambient temperature, liming may take from 10 to 30 days. After the liming process, calcium hydroxide has to be removed from the calcimine. This is

Correspondence concerning this article should be addressed to M. Bařinová at uhlirova@fai.utb.cz.

accomplished by decantation washing in water in several steps, followed by chemical deliming, and further decantation washing of the neutral calcium salt. Chemical deliming is performed because a certain amount of calcium hydroxide is held in the calcimine by a chemical bond, this amount cannot be removed by plain water washing.

From the environmental protection point of view, chemical deliming is the most important stage of the entire deliming process. During this stage, strongly bound calcium hydroxide—present in the calcimine in the form of calcium collagenate—reacts with an acid deliming agent to form a neutral calcium salt, which is then removed by water washing. In practice, deliming agents can be divided to ammonium based (the most common being ammonium sulphate) and non-ammonium based. After an ammonium salt application, the alkalinity of calcimine decreases from the original value of  $pH = 12$  to values ranging from 8.5 to 7.5.<sup>1</sup> Ammonium-based deliming agents are very effective and cheap but produce a large amount of ammonia that pollutes the environment.<sup>2</sup> For this reason, ammonium-based agents are currently being substituted by nonammonium alternatives which are included according to EU regulations in the category of BAT (Best Available Techniques).<sup>3</sup>

According to Koopmann<sup>4</sup> and Taylor et al.,<sup>5</sup> ammonium sulphate can be substituted by magnesium sulphate, or magnesium sulphate in combination with sulphuric or hydrochloric acid. This results in the reduction of ammonia nitrogen in sewage waters to 8% of the original level. Ammonium sulphate can also be substituted by magnesium lactate.<sup>6</sup> Substitution of ammonium sulphate by carbon dioxide appears to be another promising technology.<sup>7</sup> Deliming by carbon dioxide entails several advantages such as a substantial reduction of sewage water pollution and easy manipulation (distribution and dosage technology for carbon dioxide is simple, stable, and easy to handle and automate). From the operating cost point of view, carbon dioxide deliming technology is comparable to ammonium based agents. Carbon dioxide deliming, and other deliming agents based on the use of organic or inorganic acids (e.g., lactic or hydrochloric acids<sup>3</sup>) are nowadays being recommended as promising technologies and best alternatives for ammonium based deliming.<sup>5</sup>

Until recently, rationalization of natural polymers processing, especially of collagen type, had been performed mostly on the basis of direct experimental measurements and long-time practical experience.<sup>8</sup> This applies especially to the tanning and leather manufacturing industry, where the application of theoretical tools of chemical engineering is still rare. Production concentration, rising prices of energies, auxiliary agents and water, and especially strict environment protection requirements have forced researchers to deal with mathematical–physical description of individual operations and to reduce demanding and often expensive experimental measurements and especially their (often disputable) extrapolation to industrial practice. The papers<sup>9–11</sup> show the possibilities of a successful application of mathematical modeling in the tanning, leather manufacturing, and recycling processes. For example in,<sup>12</sup> mathematical model based on the principle of a continuous reaction<sup>13</sup> is used to solve the problem of a concentration shock, which occurs during desalination of cured hide and causes considerable damage of the collagen fine structure.

In this article, mathematical simulation of calcimine deliming is described by means of a unreacted nucleus model. This model (usually called the Stefan problem in mathematical physics, see e.g.,<sup>14</sup>) was first applied in the field of chemical engineering by Levenspiel.<sup>13</sup> Various forms of the Stefan problem are being studied intensively, however, usually in connection with the non-linear behavior of diffusion-reaction problems,<sup>15</sup> or with the scaling and fractal properties of the reaction front.<sup>16,17</sup> A numerical solution of a particular version of the Stefan problem is presented here, together with its practical application in the optimization of calcimine deliming. The methods used here are similar to the approach adopted in,<sup>18</sup> however, the model presented in<sup>18</sup> is much simpler (a semi-infinite domain, simpler boundary conditions, no moving point source, etc.) From the theoretical point of view, the main asset of our contribution lies in the boundary conditions, while most existing models assume either constant (Dirichlet) or no-flux (Neumann) boundary conditions, we allow the reaction-diffusion system to exchange mass with the surrounding bath. This allows modeling of closed systems, where the concentration of the deliming agent in the bath gradually decreases. In this way, not only savings in the deliming agent (usually hydrochloric acid) can be achieved but also a considerable decrease in the waste water burden with chlorides (the excess hydrochloric acid must be neutralized for further procedure). Moreover, we also model the production and diffusion of the neutral salt, this presents a moving point-source problem. The presented model can be used to determine the diffusion Coefficient of the neutralizing agent, and possibly of the neutral salt. The model is used here to verify various simplified approaches (see Section Effective Diffusion Coefficient of HCl) of parameters estimation. It can also serve as a basis for the optimization of the deliming technology.

## Physical Background and the Governing Equations

This model deals with the mathematical description of the process of chemical deliming of calcimine by hydrochloric acid. Calcium hydroxide  $\text{Ca(OH)}_2$  is removed from calcimine by soaking in water solution of hydrochloric acid HCl. The acid neutralizes calcium hydroxide as follows:



The reaction is assumed to proceed instantaneously, when compared with the speed of diffusion of the acid into the hide samples. Consequently, the regions of the calcimine already reached by the diffusing acid contain no hydroxide. The line of the hydroxide-acid boundary moves from the surface of the sample towards the center. When the boundary reaches the center of the sample, the process continues by molecular diffusion of  $\text{CaCl}_2$  out of the sample and molecular diffusion of HCl into the sample. These two chemicals are assumed not to interfere or react with each other.

For simplicity, we assume here that the calcimine samples have the form of sheets. The sheets have a uniform thickness of  $2b$  (m). This allows us to use one-dimensional representation with the independent space variable being the sample cross-section. We further use the apparent symmetry of the

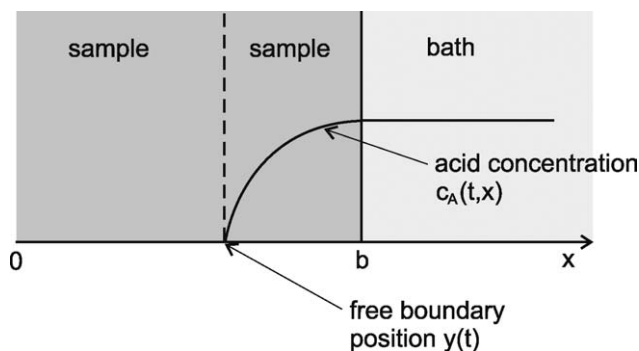


Figure 1. The geometry of the model.

concentration field inside the sample and restrict ourselves to one half of the cross-section (see Figure 1).

At time  $t = 0$ , the sample contains calcium hydroxide at a given concentration  $c_{HP}$ . This concentration is assumed to be constant throughout the sample. The sample is placed into a bath containing water solution of hydrochloric acid. The bath is well-stirred thus we assume no concentration gradients outside the sample. Consequently, concentration of all the chemicals in the surrounding bath is a function of time only. We further suppose that the concentration of any chemical on the boundary of the sample at each moment is equal to its concentration in the bath multiplied by the porosity of the sample. The velocity of the free acid-hydroxide boundary is proportional to the flux of the acid across the free boundary.

For clarity of notation, we use the subscript H (hydroxide) for calcium hydroxide, subscript A (acid) for hydrochloric acid and subscript S (salt) for calcium chloride. Let us denote by  $c_H(t, x)$  (or  $c_A(t, x)$  or  $c_S(t, x)$ , respectively) the concentration ( $\frac{\text{kg}}{\text{m}^3}$ ) of the hydroxide (or acid, or chloride, respectively) at point  $x \in (0, b)$  of the sample and time  $t \in (0, \infty)$ . Denote by  $\bar{c}_H(t)$  (or  $\bar{c}_A(t)$  or  $\bar{c}_S(t)$ , respectively) the concentrations of the respective chemicals in the bath at time  $t$ . Denote further by  $y(t)$  the position of the free acid-hydroxide boundary at time  $t \in (0, \infty)$ . For simplicity, we further assume that there is a surplus of acid in the bath, so that all the hydroxide in the sample will eventually be neutralized. Denote by  $T$  the time when the acid-hydroxide boundary reaches the centre of the sample. To prevent the model from getting too complicated, we shall ignore diffusion of the hydroxide inside the sample. The concentration field of the hydroxide can thus be modeled in the following way:

$$\begin{aligned} c_H(t, x) &= c_{HP} & \text{for } t \in (0, T) \text{ and } x \in (0, y(t)), \\ c_H(t, x) &= 0 & \text{for } t \in (0, T) \text{ and } x \in (y(t), b), \\ c_H(t, x) &= 0 & \text{for } t \in (T, \infty) \text{ and } x \in (0, b), \\ \bar{c}_H(t) &= 0 & \text{for } t \in (0, \infty), \end{aligned}$$

where  $c_{HP}$  denotes the initial concentration of the hydroxide in the sample ( $c_H$  and  $\bar{c}_H$  are defined above).

Diffusion of the acid inside the sample (between the free boundary and the sample surface) is modeled by the equation

$$\partial_t c_A(t, x) = D_A \partial_x^2 c_A(t, x) \quad \text{for } t \in (0, \infty) \text{ and } x \in (y(t), b), \quad (2)$$

where  $D_A$  ( $\frac{\text{m}^2}{\text{s}}$ ) denotes the diffusion coefficient of the acid. All the acid reaching the free boundary is neutralized by the hydroxide. Thus the boundary condition at the acid-hydroxide boundary, that is, the moving boundary, is

$$c_A(t, y(t)) = 0 \quad \text{for } t \in (0, T), \quad (3)$$

where  $T$  denotes the time when the free boundary reaches the center of the sample. When this happens, Eq. 3 is replaced by the requirement of the symmetry of the concentration field inside the sample

$$\partial_x c_A(t, 0) = 0 \quad \text{for } t \in (T, \infty). \quad (4)$$

The acid concentration on the surface of the sample is related to its concentration in the bath by the compatibility condition

$$c_A(t, b) = \varepsilon \bar{c}_A(t) \quad \text{for } t \in (0, \infty), \quad (5)$$

where  $\varepsilon[1]$  denotes the porosity of the sample boundary. The porosity is assumed a constant. The flux of the acid across the surface of the sample results in the decrease of the acidity of the bath. The mass balance of the acid in the bath leads to

$$\frac{1}{2} V_0 \partial_t \bar{c}_A(t) + D_A S \partial_x c_A(t, b) = 0 \quad \text{for } t \in (0, \infty). \quad (6)$$

where  $V_0$  ( $\text{m}^3$ ) stands for the volume of the bath and  $S$  ( $\text{m}^2$ ) denotes the surface area of one side of the hide sample. (The factor  $\frac{1}{2}$  is due to axisymmetry.) The initial concentration of the acid in the bath is given by

$$\bar{c}_A(0) = \bar{c}_{AP}. \quad (7)$$

The flux  $F(t)$  ( $\frac{\text{kg}}{\text{s}}$ ) of the acid across the free boundary into the core of the sample at time  $t$  is given by

$$F(t) = D_A S \partial_x c_A(t, y(t)). \quad (8)$$

This means the flux of

$$\frac{F(t)dt}{M_A}$$

moles of the acid during time interval  $dt$ , where  $M_A$  ( $\frac{\text{kg}}{\text{mol}}$ ) denotes the molar mass of the acid. All this mass is “consumed” in the neutralization of the hydroxide according to the reaction scheme (1), thus

$$\frac{F(t)dt}{2M_A} \quad (9)$$

moles of calcium hydroxide are consumed, which corresponds to

$$\frac{M_H F(t)dt}{2M_A} \quad (10)$$

kilograms. Here  $M_H$  ( $\frac{\text{kg}}{\text{mol}}$ ) denotes the molar mass of the hydroxide. If we assume that the concentration  $c_{HP}$  of the

hydroxide is constant throughout the sample, the calculated consumption corresponds to the shift of the acid-hydroxide boundary by

$$dy = \frac{M_H F(t)}{2M_{A\text{CHPS}}} dt \quad (11)$$

meters during the time interval  $dt$ . Expressing  $dy/dt$  from Eq. 11 and substituting for  $F(t)$  from (8), the velocity of the free boundary is given by

$$\partial_t y(t) = \frac{dy}{dt}(t) = -\frac{M_H D_A}{2M_{A\text{CHPS}}} \partial_x c_A(t, y(t)) \quad \text{for } t \in (0, T), \quad (12)$$

where  $T$  again denotes the time when the free boundary reaches the centre of the sample. When this happens, Eq. 12 is replaced by the obvious terminal state

$$y(t) = 0 \quad \text{for } t \in (T, \infty). \quad (13)$$

Recall that the free boundary moves toward the centre of the sample, thus  $\partial_t y < 0$ , whence the negative sign in Eq. 12. The initial condition for the free boundary reads

$$y(0) = b. \quad (14)$$

The initial condition for the acid concentration in the sample is zero.

Diffusion of calcium chloride inside the sample is modeled by the equation

$$\partial_t c_S(t, x) = D_S \partial_x^2 c_S(t, x) + P(t, x) \quad \text{for } t \in (0, \infty) \quad \text{and} \quad x \in (0, b), \quad (15)$$

where  $D_S(\frac{\text{m}^2}{\text{s}})$  denotes the diffusion coefficient of the chloride and  $P(t, x)(\frac{\text{kg}}{\text{m}^3 \text{s}})$  stands for the production term. Here, we assume that the chloride is perfectly soluble and interacts neither with the acid, nor with the hydroxide. By an analogy to the derivation of the hydroxide consumption term, one easily finds that the production of  $\text{CaCl}_2$  at point  $y(t)$  during time  $dt$  is equal to

$$G(t) = \frac{M_S F(t) dt}{2M_A}$$

kilograms, where  $M_S(\frac{\text{kg}}{\text{mol}})$  denotes the molar mass of the chloride. Substituting from (8) and (11), we obtain

$$G(t) = -\frac{S_{\text{CHP}} M_S dt}{M_H} \partial_t y(t).$$

This production is concentrated into the (infinitesimally) thin region of the free boundary  $(y(t), y(t) + dx) \times S$ . Consequently, the rate of the production of the chloride  $(\frac{\text{kg}}{\text{m}^3 \text{s}})$  converges in the continuous limit ( $dx \rightarrow 0$ ) to

$$P(t, x) = -\frac{c_{\text{HP}} M_S}{M_H} \partial_t y(t) \delta[y(t)](x), \quad (16)$$

where  $\delta(y)$  is the Dirac delta function centered at  $y$  defined by

$$\delta[y](x) = \begin{cases} \infty & \text{for } x = y, \\ 0 & \text{for } x \neq y, \end{cases}$$

Note that the dimension of  $\delta$  is  $(\text{m}^{-1})$  because  $\int_{\mathbb{R}} \delta[y](x) dx = 1$ . Also note that  $P(t, x) \equiv 0$  for  $t \in (T, \infty)$  because  $\partial_t y(t) = 0$  after the free boundary has reached the center of the sample.

The initial conditions are

$$c_S(0, x) = 0 \quad \text{and} \quad \bar{c}_S(0) = 0 \quad (17)$$

The symmetry of the concentration field in the sample is again reflected by (see Eq. 4)

$$\partial_x c_S(t, 0) = 0 \quad \text{for } t \in (0, \infty). \quad (18)$$

The flux of the chloride across the boundary of the sample is again modeled by the equation (see Eq. 6)

$$\frac{1}{2} V_0 \partial_t \bar{c}_S(t) + D_S S \partial_x c_S(t, b) = 0 \quad \text{for } t \in (0, \infty). \quad (19)$$

Compatibility of the concentration across the boundary is ensured by (see Eq. 5)

$$c_S(t, b) = \varepsilon \bar{c}_S(t) \quad \text{for } t \in (0, \infty). \quad (20)$$

## Dimensionless Formulation

It is convenient to express the above derived model in dimensionless variables. However, we need to be careful here: The dimensionless time is usually measured in terms of the speed of diffusion, the Fourier criterion reads

$$Fo = \frac{Dt}{b^2}$$

which poses the problem of which diffusion coefficient ( $D_A$  or  $D_S$ ) to take for  $D$ . We choose the first one, which implies that the Fourier criterion will retain its physical meaning only for the description of the acid concentration field.

Let us define the dimensionless quantities in the following usual way:

$$X = \frac{x}{b} \quad \text{and} \quad Fo = \frac{D_A t}{b^2}.$$

Consequently, the domains change according to the following scheme:

$$x \in (0, b) \longrightarrow X \in (0, 1),$$

and

$$t \in (0, T) \longrightarrow Fo \in (0, \mathcal{F}) \quad t \in (T, \infty) \longrightarrow Fo \in (\mathcal{F}, \infty),$$

where  $\mathcal{F} = \frac{D_A T}{b^2}$  stands for the dimensionless terminal time of the free boundary movement. The dimensionless concentration

fields are defined as follows:

$$C_I(Fo, X) = \frac{c_I(t, x)}{c_{HP}} \quad \text{and} \quad \bar{C}_I(Fo) = \frac{\varepsilon \bar{c}_I(t)}{c_{HP}},$$

where I stands either for A, H or S, as required. Observe that all the dimensionless concentration fields arise by dividing the real-world concentrations by the same value  $c_{HP}$  which may result in values exceeding the unity. Although this may be unusual, it is practical for easy comparison of the three dimensionless concentration fields. The dimensionless position of the free boundary is defined by

$$Y(Fo) = \frac{y(t)}{b}.$$

Rewriting Eqs. 2–6 in the dimensionless variables, we obtain

$$\partial_{Fo} C_A(Fo, X) = \partial_X^2 C_A(Fo, X) \quad \text{for } Fo \in (0, \infty) \quad \text{and} \quad X \in (Y(Fo), 1), \quad (21)$$

$$C_A(Fo, Y(Fo)) = 0 \quad \text{for } Fo \in (0, \mathcal{F}), \quad (22)$$

$$\partial_X C_A(Fo, 0) = 0 \quad \text{for } Fo \in (\mathcal{F}, \infty), \quad (23)$$

$$C_A(Fo, 1) = \bar{C}_A(Fo) \quad \text{for } Fo \in (0, \infty), \quad (24)$$

$$\partial_{Fo} \bar{C}_A(Fo) + N_1 \partial_X C_A(Fo, 1) = 0 \quad \text{for } Fo \in (0, \infty), \quad (25)$$

$$\bar{C}_A(0) = \bar{C}_{AP} \quad (26)$$

with

$$N_1 = \frac{\varepsilon V}{V_0} \quad \text{and} \quad \bar{C}_{AP} = \frac{\varepsilon \bar{c}_{AP}}{c_{HP}},$$

where  $V$  ( $\text{m}^3$ ) denotes the volume of the sample. The dimensionless free boundary motion is given by

$$\partial_{Fo} Y(Fo) = -\frac{M_H}{2M_A} \partial_X C_A(Fo, Y(Fo)) \quad \text{for } Fo \in (0, \mathcal{F}), \quad (27)$$

with  $Y(0) = 1$  and  $Y(Fo) = 0$  for  $Fo \in (\mathcal{F}, \infty)$ .

Diffusion of the calcium chloride (Eqs. 15, 17–20) transform to the dimensionless variables as follows: (Note that  $\delta[y(t)](x) = \frac{1}{b} \delta[Y(Fo)](X)$ )

$$\partial_{Fo} C_S(Fo, X) = \frac{D_S}{D_A} \partial_X^2 C_S(Fo, X) - \frac{M_S}{M_H} (\partial_{Fo} Y(Fo)) \delta[Y(Fo)](X) \quad \text{for } Fo \in (0, \infty) \quad \text{and} \quad X \in (0, 1), \quad (28)$$

$$C_S(0, X) = 0 \quad \text{for } X \in (0, 1), \quad (29)$$

$$\bar{C}_S(0) = 0 \quad (30)$$

$$\partial_X C_S(Fo, 0) = 0 \quad \text{for } Fo \in (0, \infty), \quad (31)$$

$$C_S(Fo, 1) = \bar{C}_S(Fo) \quad \text{for } Fo \in (0, \infty), \quad (32)$$

$$\partial_{Fo} \bar{C}_S(Fo) + N_2 \partial_X C_S(Fo, 1) = 0 \quad \text{for } Fo \in (0, \infty), \quad (33)$$

with

$$N_2 = \frac{\varepsilon V D_S}{V_0 D_A} = \frac{D_S}{D_A} N_1.$$

## Numerical Solution

In order to find the numerical solution of the model above, we use the finite difference explicit scheme and discretize both the dimensionless space and time variables. We use a version of the standard front-tracking method.<sup>18</sup>

In each time step, we first move the free boundary (Eq. 27). The time-derivative is approximated by a forward difference

$$\partial_{Fo} Y(Fo) \sim \frac{[Y]^{k+1} - [Y]^k}{dFo},$$

where  $Y^k$  denotes the position of the free boundary at  $k$ -th dimensionless time level and  $dFo$  stands for the length of the discretization step. The derivative of the concentration field at point  $Y(Fo)$  is approximated by the difference

$$\partial_X C_A(Fo, Y(Fo)) \sim \frac{[C_A]_{Y_{\text{pos}+1}}^k - [C_A]_{Y_{\text{pos}}}^k}{dX},$$

where  $[C_A]_{Y_{\text{pos}}}^k$  stands for the value of the dimensionless concentration of the acid on the  $k$ -th dimensionless time level at the node  $Y_{\text{pos}}$  – the discretized position of the free boundary. Thus, the position of the free boundary is also discretized to fit the a-priori division of the interval (0,1).

Next, new values of the surrounding concentrations  $\bar{C}_A$  and  $\bar{C}_S$  are computed (Eqs. 25 and 33). The fluxes of the respective substances across the boundaries are again approximated by forward differences, as above. Then, new values of  $C_A$  and  $C_S$  on the boundaries are set (Eqs. 24 and 32).

Next, one step of diffusion is performed, both for the acid and for the chloride, on the appropriate domains (Eqs. 21 and 28). The first derivative with respect to time is again approximated by a forward difference and the second derivative with respect to space is approximated by a second order central difference

$$\partial_X^2 C_A(Fo, X) \sim \frac{[C_A]_{l-1}^k - 2[C_A]_l^k + [C_A]_{l+1}^k}{dX^2},$$

where  $[C_A]_l^k$  denotes the value of  $C_A$  on the  $k$ -th time level at the  $l$ -th node of the division of the interval (0,1). In the production term in Eq. 28, the Dirac delta function centered at  $Y(Fo)$  is approximated by

$$\delta[Y(Fo)] \sim \frac{\text{char}[Y, dX]}{dX},$$

where  $\text{char}(Y, dX)$  stands for the characteristic function of the interval  $(Y, Y + dX)$ . This approximation is represented by a



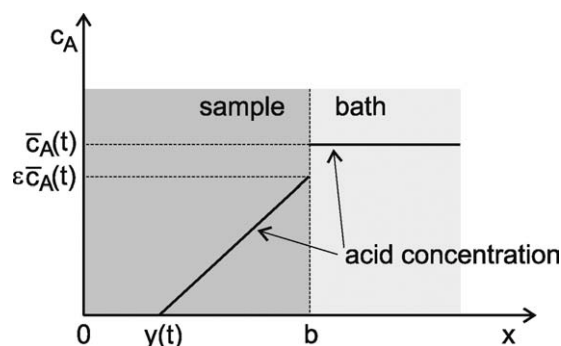


**Figure 2. The assumption of linearity of the acid concentration field.**

The term  $y(t)$  denotes the position of the free acid-hydroxide boundary, and  $b$  denotes half of the sample cross-section. The values of concentration across the boundary satisfy the compatibility condition (5). Compare to Figure 6.

vector of zeros with a single nonzero entry of value  $\frac{1}{dX}$  at the position  $Y_{pos}$ .

This time loop proceeds until the free boundary reaches the centre of the sample. Then, either the modeling stops or plain diffusion of  $\text{CaCl}_2$  follows, which is trivial from the numerical point of view.

To start this numerical process, we cannot begin with  $Y(0) = 1$ , because this would result in simulating the first step of the diffusion on an empty set. We therefore set  $Y(0) = 1 - dX$  and prescribe  $C_A(0,1) = \bar{c}_A$  and  $C_A(0,1 - dX) = 0$ . This represents an artificial additional amount of acid in the system, which is, however, negligible for  $dX$  small enough.

## Experimental

In this section, we describe the experimental methods used to measure or estimate the numerical values of the parameters of the model.

### Initial concentration of calcium hydroxide in calcimine

Several samples of calcimine of masses ranging from 2 to 5 grams were sliced and neutralized by boiling in diluted 1:1 hydrochloric acid. After the sample had dissolved, the solution was diluted and the concentration of calcium was measured by direct atomic adsorption.

The initial concentration  $c_{HP}$  of  $\text{Ca}(\text{OH})_2$  in the calcimine was found to be approximately  $30 \left(\frac{\text{kg}}{\text{m}^3}\right)$ .

### Porosity

The porosity of calcimine was estimated by squeezing or centrifuging the samples. It can be assumed that this process removes all the water from the calcimine pores, allowing the estimation of the porosity.

In this way, the porosity was estimated to be  $\sim 50\%$ , thus  $\varepsilon = 0.5$ .

### Effective diffusion coefficient of HCl

Let us assume again that the diffusion coefficient is small enough. Then we can assume that the concentration field of the acid inside a calcimine sample (between the acid-hydroxide boundary and the surface of the sample) is linear (see Figure 2). See also Figure 6 where the full solution of the model is shown, observe that the departure from linearity is not fundamental.

This assumption of linearity simplifies Eq. 12 (velocity of the free boundary) substantially because the gradient of the field  $c_A$  can be expressed in the following way

$$\partial_x c_A(t, y(t)) \sim \frac{\varepsilon \bar{c}_A}{b - y(t)}.$$

With this approximation, Eq. 12 simplifies to

$$\partial_t y(t) = -\frac{M_H D_A}{2M_A c_{HP}} \frac{\varepsilon \bar{c}_A}{b - y(t)}, \quad (34)$$

(where we remind that  $M_A$  and  $M_H$  stand for the molar masses of HCl and  $\text{Ca}(\text{OH})_2$ , respectively,  $c_{HP}$  denotes the initial concentration of the hydroxide in the sample,  $\bar{c}_A$  the concentration of the acid in the surrounding bath, and  $\varepsilon$  the porosity of the sample.) Denote

$$L := \frac{M_H}{2M_A} \frac{\varepsilon \bar{c}_A}{c_{HP}}$$

and introduce a new variable

$$z(t) = b - y(t)$$

so that

$$z'(t) = -y'(t).$$

Then Eq. 34 reads

$$z'(t) = \frac{LD_A}{z} \quad \text{with} \quad z(0) = 0.$$

This differential equation can be solved explicitly to obtain

$$z(t) = \sqrt{2LD_A t}. \quad (35)$$

This suggests that the dependence of  $z(t)$  on  $\sqrt{t}$  is linear and its slope can be estimated by the least squares method from observation of the free boundary movement. Then we can estimate the value of  $D_A$  by

$$D_A = \frac{k^2}{2L} = \frac{M_A}{M_H} \frac{k^2 c_{HP}}{\varepsilon \bar{c}_A}, \quad (36)$$

where  $k$  denotes the slope of the linear dependence of  $z(t)$  on  $\sqrt{t}$ .

In the experimental setup, a sample of calcimine with the initial concentration of calcium hydroxide of  $c_{HP} = 30 \left(\frac{\text{kg}}{\text{m}^3}\right)$  was prepared. The porosity of the sample was again  $\varepsilon = 0.5$ . The sample was placed into a 0.7% solution of HCl (thus,  $\bar{c}_A = 7 \left(\frac{\text{kg}}{\text{m}^3}\right)$ ). In regular time intervals, a slice 1 cm thick was cut off the sample and taken out of the bath. The slice

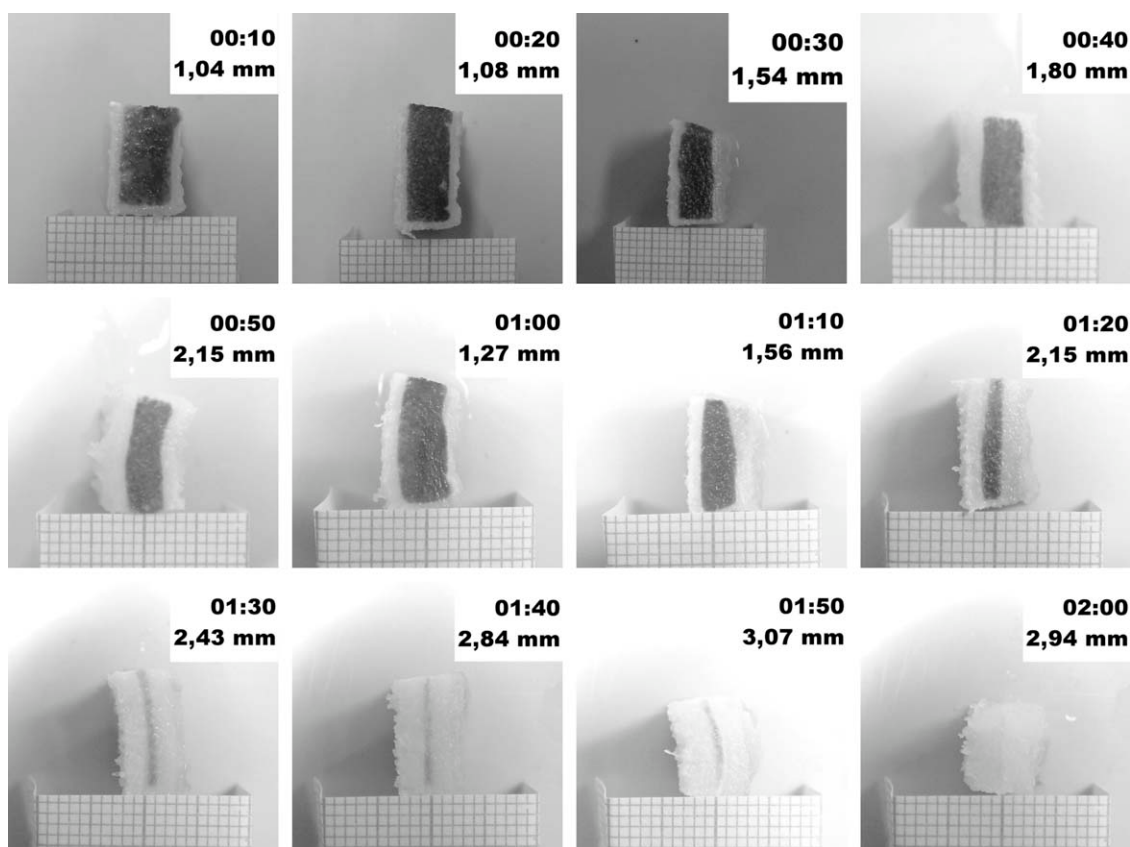


Figure 3. The evolution of the acid-hydroxide free boundary.

was quickly brushed with an ethanol solution of phenolphthalein and photographed (see Figure 3).

The linear regression of  $z(t)$  against  $\sqrt{t}$  (see Figure 4) provides the estimate

$$k = 0.2566 \frac{\text{mm}}{\sqrt{\text{min}}}$$

with the confidence interval being (0.1872, 0.3260). This makes

$$k^2 = 1.10 \times 10^{-9} \frac{\text{m}^2}{\text{s}},$$

and, according to (36),

$$D_A = 4.64 \times 10^{-9} \frac{\text{m}^2}{\text{s}}.$$

## Results

Let us now perform the numerical solution of the model using the estimated data. The following parameters were used:

$$D_A = 4.64 \times 10^{-9} \frac{\text{m}^2}{\text{s}}, \quad D_S = 3 \times 10^{-10} \frac{\text{m}^2}{\text{s}}, \\ \varepsilon = 0.5, \quad b = 0.005 \text{ m},$$

$$V = 5 \text{ m}^3, \quad V_0 = 5 \text{ m}^3, \quad \bar{c}_{\text{AP}} = 100 \frac{\text{kg}}{\text{m}^3}, \quad c_{\text{HP}} = 30 \frac{\text{kg}}{\text{m}^3}, \\ M_H = 74.1 \frac{\text{kg}}{\text{kmol}}, \quad M_A = 36.5 \frac{\text{kg}}{\text{kmol}}, \quad M_S = 111 \frac{\text{kg}}{\text{kmol}}.$$

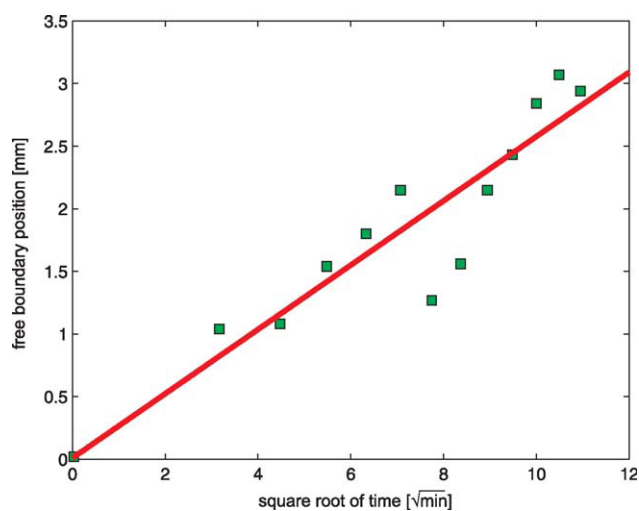
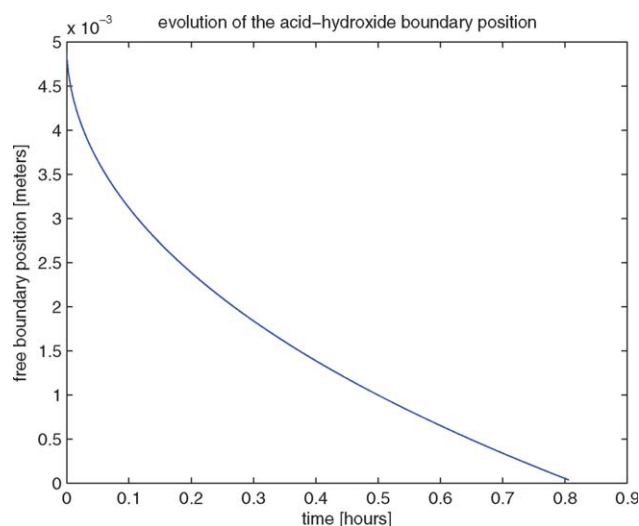


Figure 4. Linear regression: Estimation of the slope of the linear dependence of  $z(t)$  on  $\sqrt{t}$ .

(Color figure can be viewed in the online issue, which is available at [www.interscience.wiley.com](http://www.interscience.wiley.com).)



**Figure 5. Evolution of the free boundary position (its distance from the center of the sample).**

The boundary separates hydroxide-soaked core of the sample from the already neutralized outer layer. (Color figure can be viewed in the online issue, which is available at [www.interscience.wiley.com](http://www.interscience.wiley.com).)

The diffusion coefficient  $D_S$  of  $\text{CaCl}_2$  was estimated using the Nernst-Haskell equation<sup>19</sup> with the use of the values of limiting ionic conductance for cations and anions from the *Chemical Engineer's Handbook*.<sup>20</sup> This makes the dimensionless constants equal

$$N_1 = \frac{1}{2}, \quad N_2 = 3.2328 \times 10^{-2}, \quad \bar{C}_{AP} = \frac{5}{3},$$

$$\frac{D_S}{D_A} = 6.4655 \times 10^{-2}, \quad \frac{M_S}{M_H} = 1.4980.$$

The parameters of the discretization were chosen to be

$$dX = 5 \times 10^{-3}, \quad dF = 2 \times 10^{-6}.$$

This corresponds to the division of the interval (0, 1) into 200 segments each 0.025 mm of real length. The time step corresponds approximately to 0.01 sec. The results of the numerical model are shown in Figures 5–7.

## Discussion and Conclusions

It has been shown that even such complex processes as transport of chemicals in a natural polymer accompanied by a chemical reaction allow a reasonable mathematical description. The mathematical model allows the prediction of  $T$  (the terminal time when the acid reaches the center of the sample). However, calibration of the model on real data would be needed (the values of the  $D_A$  and  $D_S$  need to be fitted). This was not the purpose of this article. On the other hand, we have shown that this full model justifies the usage of a simplified way to determine the effective diffusion coefficient (see Section Effective Diffusion Coefficient of HCl). The values of the coefficient  $D_A$  calculated from the experimental data by means of the simplified model are comparable with the values calculated for an infinite dilution according to the Nernst-Haskell equation<sup>19</sup> with the use of the val-

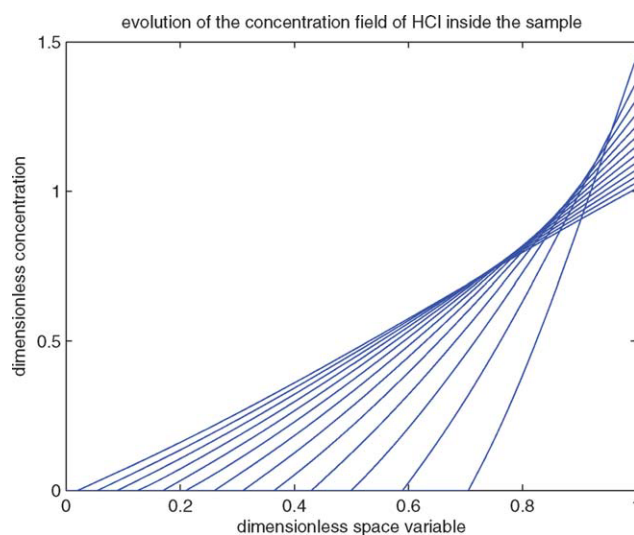


**Figure 6. Evolution of the HCl concentration field inside the sample. The position of the moving free boundary is indicated by the zero values of the concentration.**

The dimensionless time-interval between successive lines is 0.04 which corresponds approximately to 3.6 min. The fields with smaller gradients correspond to later times, thus time “increases from the right to the left”. (Color figure can be viewed in the online issue, which is available at [www.interscience.wiley.com](http://www.interscience.wiley.com).)

ues of limiting ionic conductance for cations and anions from the *Chemical Engineer's Handbook*;<sup>20</sup> the calculated value is equal to  $3.31 \times 10^{-9} \left(\frac{\text{m}^2}{\text{s}}\right)$ .

To control the deliming process, it is necessary to be able to experimentally track the acido-basic boundary as well as

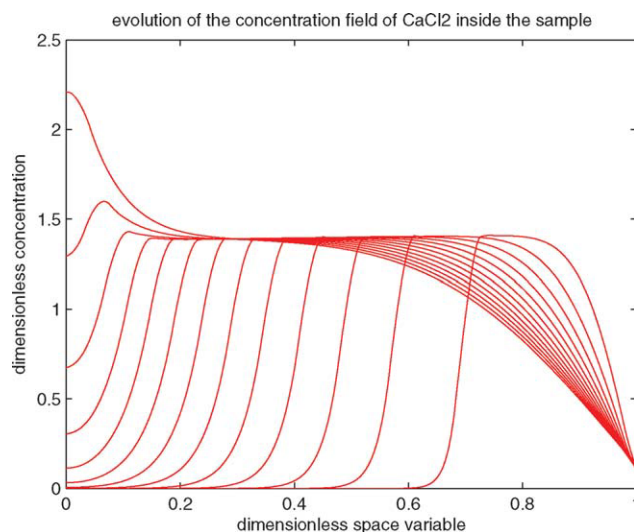


**Figure 7. Evolution of the  $\text{CaCl}_2$  concentration field inside the sample.**

The position of the moving free boundary is indicated by the peaks which correspond to the production of the salt at the point of the contact of the acid with the hydroxide (at the free boundary). The dimensionless time-interval between successive lines is 0.04 which corresponds to 3.6 min. As time increases, the peaks move toward the center of the sample. (Color figure can be viewed in the online issue, which is available at [www.interscience.wiley.com](http://www.interscience.wiley.com).)



the concentrations of the reacting chemicals, the deliming agent (HCl in our case) and the neutral salt (CaCl<sub>2</sub>). In practice, it is required that water pollution is minimized. The proposed mathematical model helps us to keep all these aspects and parameters under control. For example, evolution of the acido-basic boundary presented in Figure 5 shows the course of the transformation of alkalic calcimine into an acidic region. This is necessary for acidic swelling which enables optimal extrusion, for example, in the production of biodegradable sheets. The model may provide information about the time-dependence of the reaction, thus enabling us to estimate the final production of swollen calcimine. Optimal reaction time is given by two mutually opposite constraints; on one hand, the deliming process is required to proceed quickly, which demands higher concentrations of the deliming agent, on the other hand, high concentrations of the deliming agent result in the production of undesirable neutral salts which pollute the waste waters. Rationalization of the deliming process means the search for the equilibrium between the two above mentioned constraints and the presented mathematical model together with its numerical solution can serve as a basis for the achievement of this equilibrium.

The quantitative description is general enough, so that any deliming agent (the most commonly used are mentioned in the Introduction) can be used. Deliming with hydrochloric acid (modeled here) is an example of a nonammonium based deliming process. The advantage of this technology is especially low price of the chemical; however, the technology brings a major environmental problem concerning an extensive burden of waste water contaminated with chlorides. It is necessary to minimize the consumption of hydrochloric acid in the deliming process so that the concentration of chlorides does not exceed the limits allowed by national or international regulations. The presented model can also be used as a basis for such optimization.

To avoid the pollution of waste waters with chloride anions, other deliming agents can be used such as lactic acid, which is, however, considerably more expensive. The consumption of lactic acid then needs to be minimized. In this case, the cleaning (dechlorination) costs and the deliming agent price represent the two competing constraints. In practice, our results were applied in the deliming of white hide in commercial tanneries,<sup>21</sup> however, the optimization process was mainly based on long-time practical experience. The mathematical model, its numerical solution and its consequences are presented here for the first time. Optimization of the production of high-quality gelatin and biodegradable sheets based on the presented model is currently being used by a commercial company.

## Acknowledgments

This work was supported by the Council of Czech Government (MSM 619 895 9214), and the Ministry of Education of the Czech Republic (MSM 7088352102).

## Notation

$t$  = time (s)  
 $x$  = space/position (m)

$b$  = half-thickness of the sample (m)  
 $c_1(t, x)$  = concentration of substance I inside the sample. I stands for A (hydrochloric acid), H (calcium hydroxide), or S (calcium chloride), as required.  
 $\bar{c}_1(t)$  = concentration of substance I in the bath (I has the same meaning as above) ( $\frac{\text{kg}}{\text{m}^3}$ )  
 $D_1$  = effective diffusion coefficient of substance I ( $\frac{\text{m}^2}{\text{s}}$ )  
 $M_1$  = molar mass of substance I ( $\frac{\text{kg}}{\text{mol}}$ )  
 $y(t)$  = position of the acid-hydroxide interface, that is, the free boundary position (m)  
 $T$  = the terminal time (when the free boundary reaches the center of the sample) (s)  
 $\varepsilon$  = porosity of the sample surface (1)  
 $V_0$  = volume of the bath ( $\text{m}^3$ )  
 $V$  = volume of the sample ( $\text{m}^3$ )  
 $S$  = surface area of the sample ( $\text{m}^2$ )  
 $\bar{c}_{\text{AP}}$  = initial concentration of the hydrochloric acid in the bath ( $\frac{\text{kg}}{\text{m}^3}$ )  
 $F(t)$  = flux of the hydrochloride acid across the free boundary ( $\frac{\text{kg}}{\text{s}}$ )  
 $c_{\text{HP}}$  = initial concentration of the calcium hydroxide in the sample ( $\frac{\text{kg}}{\text{m}^3}$ )  
 $P(t, x)$  = rate of production of calcium chloride in the sample ( $\frac{\text{kg}}{\text{m}^3 \cdot \text{s}}$ )  
 $\delta(y)(x)$  = Dirac's  $\delta$ -function centered at  $y$  ( $\frac{1}{\text{m}}$ )  
 $Na$  = soaking number (1)  
 $Fo$  = dimensionless time (1)  
 $X$  = dimensionless position (1)  
 $C_1, \bar{C}_1$  = dimensionless version of  $c_1$  and  $\bar{c}_1$  (1)  
 $\mathcal{F}$  = dimensionless version of  $T$  (1)  
 $Y$  = dimensionless version of  $y$  (1)  
 $dX$  = dimensionless space discretization step (1)  
 $dFo$  = dimensionless time discretization step (1)  
 $L, G, N_1, N_2, z, k$  = auxiliary variables  
 $\partial_t, \partial_x, \partial_{Fo}, \partial_X$  = partial derivatives  
 $[Y]_l^k$  = discretized quantity  $Y$  evaluated at the  $k$ -th time level at node  $l$ .

## Literature Cited

- Constantin JM. Comparative evaluation of deliming by the EPA (Koopman) epsom salts and ammonium sulfate processes. *J Am Leather Chem Assoc.* 1981;76:40–45.
- Rossin AC, Perry R, Lester JN. Removal of zeolite type during primary sedimentation and its effect on metal removal. *Water Research.* 1982;16:1223–1232.
- Korenek Z, Ludvik J. Non-ammonium based deliming. The present situation. (in Czech) *Kozarstvi.* 1992;42:11–15.
- Koopman RC. Deliming with epsom salts. *J Am Leather Chem Assoc.* 1982;77:358–364.
- Taylor MM, Diefendorf EJ, Civitillo Sweeney PM, Fearheller SH, Bailey DG. Wet process technology IV. Evaluation of an alternative deliming agent. *J Am Leather Chem Assoc.* 1988;83:35–41.
- Kolomaznik K, Blaha A, Bailey DG, Taylor MM, Dedrle T. Non-ammonia deliming of cattle hides with magnesium lactate. *J Am Leather Chem Assoc.* 1996;91:18–20.
- Sunahara M, Hozan D, Chonan Y. Carbon dioxide deliming technology in pig leather production. *Hikaku Kagaku.* 1999;44:273–280.
- Corning DR. The Chemical Engineer in the Tannery. *J Soc Leather Technol Chem.* 1972;56:95–102.
- Hernandez Balada E, Marmer WN, Kolomaznik K, Cooke PH, Dudley RL. Mathematical model of raw hide curing with brine. *J Am Leather Chem Assoc.* 2008;103:167–173.
- Kolomaznik K, Vasek V, Zelinka I, Mladek M, Langmaier F. Automatic control of recycling technology for chromium from liquid and solid tannery waste. *J Am Leather Chem Assoc.* 2005;100:119–123.
- Kolomaznik K, Prokopova Z, Vasek V, Bailey DG. Development of a control algorithm for the optimized soaking of cured hides *J Am Leather Chem Assoc.* 2006;101:309–316.

12. Kolomaznik K, Furst T, Uhlirova M. Relationship between mass transport and the quality of cured hide. *Can J Chem Eng.* 2009;87:60–68.
13. Levenspiel O. *Chemical Reaction Engineering*, 3rd ed. New York: John Wiley, 1999.
14. Rubenstein LI. *The Stefan Problem*. Providence; R.I: American Mathematical Society, 1971.
15. Karma A, Rappel WJ. Phase-field method for computationally efficient modeling of solidification with arbitrary interface kinetics. *Phys Rev E.* 1996;53:3017–3020.
16. Chopard B, Droz M, Magnin J, Racz Z. Localization-delocalization transition of a reaction-diffusion front near a semipermeable wall. *Phys Rev E.* 1997;56:5343–5350.
17. Goriely A. Simple solution to the nonlinear front problem. *Phys Rev Letters.* 1995;75:2047–2050.
18. Reverberi AP, Scalas E, Veglio F. Numerical solution of moving boundary problems in diffusion processes with attractive and repulsive interactions. *J Phys A Math Gen.* 2002;35:1575–1588.
19. Reid RC, Prausnitz JM, Sherwood TK. *The Properties of Gases and Liquids*. New-York: McGraw-Hill, 1977.
20. Perry HR, Chilton CH, editors. *Chemical Engineers' Handbook*. New York: McGraw-Hill, 1973.
21. Kolomaznik K, Bailey D, Taylor M. Deliming of un-bonded lime from white hide. *J Am Leather Chem Assoc.* 2007;102:158–163.

*Manuscript received Feb. 9, 2009, and revision received Aug. 6, 2009.*